Resonant Excitation of Disk Oscillations in Deformed Disks II: A Model of High Frequency QPOs

Shoji KATO

2-2-2 Shikanodai-Nishi, Ikoma-shi, Nara 630-0114

kato.shoji@gmail.com; kato@kusastro.kyoto-u.ac.jp

Abstract

The amplification of disk oscillations resulting from nonlinear resonant couplings between the oscillations and a disk deformation is examined. The disk is geometrically thin and general relativistic with a non-rotating central source. A Lagrangian formulation is adopted. The author examined the same problem a few years ago, but here we derive a general stability criterion in a more perspective way. Another distinct point from the previous work is that in addition to the case where the deformation is a warp, the case where the deformation is a one-armed pattern symmetric with respect to the equatorial plane is considered. The results obtained show that in addition to the previous results that the inertial-acoustic mode and g-mode oscillations are amplified by horizontal resonance in warped disks, they also amplified by horizontal resonance in disks deformed by one-armed pattern symmetric with respect to the equatorial plane. If we consider local oscillations that are localized around boundaries of their propagation region, the resonance occurs at $4r_{\rm g}$, where $r_{\rm g}$ is the Schwarzschild radius. If nonlocal oscillations are considered, frequency ranges of oscillations where oscillations are resonantly amplified are specified.

1. Introduction

Since the discovery of high-frequency quasi-periodic oscillations (QPOs) by RXTE satellite in neutron-star X-ray and black-hole X-ray binaries, much progress has been made both in observations of the high-frequency QPOs and in their theoretical modeling. This is because the QPOs are regarded to be a very powerful tool to explore the mass and spin of the central compact sources and also to explore the physical states of the innermost relativistic region of accretion disks.

One of promising models of the high-frequency QPOs is that they are disk oscillations

resonantly excited in relativistic disks. At an early stage of observational development of the high-frequency QPOs, Abramowicz and Kluźniak (2001) and Kluźniak and Abramowicz (2001) already pointed out the importance of resonant processes as the cause of the high-frequency QPOs. Their model is that the high-frequency QPOs are the results of resonant couplings between the vertical and horizontal epicyclic oscillations in disks. This idea is very fascinating, but there seems to have still uncertainty concerning their excitation processes.

Kato (2003, 2004), on the other hand, proposed another resonant model of the high-frequency QPOs, where the QPOs are regarded to be disk oscillations resonantly excited on *deformed* disks. In this model, a deformation of disks from an axially-symmetric equilibrium state is an essential ingredient for resonant excitation of disk oscillations. He especially considered the case where the disk deformation is a warp. An outline of the model is as follows. A nonlinear coupling between a disk oscillation (hereafter we call it the original oscillation) and a warp brings about some disk oscillations (we call them intermediate oscillations). The intermediate oscillations make a resonant coupling with the unperturbed disk at some particular radius of the disk. After this resonant coupling with the unperturbed disk, the intermediate oscillations feedback to the original oscillation by nonlinearly coupling with the warp. Since the nonlinear feedback processes involve a resonance, the original oscillation is amplified or dampened. For this nonlinear coupling to occur, however, some conditions must be satisfied. These conditions specify the place(s) where the resonance occurs and the frequencies of resonant oscillations (Kato 2004). Among such resonant oscillations, some ones are amplified and others are dampened (Kato 2004). Application of these resonantly-excited oscillations to the high-frequency QPOs has been made by Kato and his collaborators, e.g., Kato and Fukue (2006) and Kato (2007).

Examination in which cases the oscillations are resonantly excited was made by Kato (2003) and (2004), but their analyses are very lengthy and mathematically not perspective. The reason is that cylindrical coordinates are introduced at a early stage of formulation. In spite of this, the results obtained are rather simple. This suggests that a more perspective and general derivation of stability criterion is possible. Really, we find that the stability criterion can be derived in a simpler and perspective way. A purpose of this paper is to show this. The results obtained confirm the stability criteria obtained by Kato (2004).

In addition, we show in this paper that a warp is not only one type of deformation that can resonantly amplify disk oscillations. One-armed deformations of disks that are symmetric with respect to the equatorial plane are also one of possible candidates that can resonantly amplify disk oscillations.

In our previous work, we specifically consider the cases where oscillations are local and localized around the boundaries of their propagation region. In this paper we relax this approximation, and specify the frequency ranges (in other words, the radial ranges) where global oscillations are resonantly amplified.

2. Summary of Basic Nonlinear Hydrodynamic Equations

Here, we summarize basic nonlinear hydrodynamic equations that are necessary to examine nonlinear resonant processes and their stability. Details are given by Kato (2004).

We are interested in general relativistic disks, since in the resonant instability processes that we consider here the general relativity is essential. The essence of the effects of the general relativity, however, can be taken into account within the framework of a pseudo-Newtonian formulation using the gravitational potential introduced by Paczyński and Wiita (1980), provided that the central object has no rotation.

The formulation presented here are quite general until some approximations are introduced later. The unperturbed state of the systems considered here is a steady equilibrium state. In Lagrangian formulation, the hydrodynamic equation describing perturbations over the state can be written as (Lynden-Bell and Ostriker 1967)

$$\frac{D_0^2 \boldsymbol{\xi}}{Dt^2} = \delta\left(-\nabla\psi - \frac{1}{\rho}\nabla p\right), \tag{1}$$

where $\boldsymbol{\xi}$ is a displacement vector associated with perturbations, and D_0/Dt is the time derivative along an unperturbed flow, $\boldsymbol{u}_0$, and is related to the Eulerian derivative, $\partial/\partial t$, by

$$\frac{D_0}{Dt} = \frac{\partial}{\partial t} + \boldsymbol{u}_0 \cdot \nabla. \tag{2}$$

In equation (1), δ represents the Lagrangian variation of the quantities in the subsequent parentheses, and ψ is the gravitational potential. Other notations in equation (1) have their usual meanings.

The basic equation (1) is valid even when the displacement $\boldsymbol{\xi}$ has a finite amplitude. The purpose here is to explicitly write down the right-hand side of equation (1) up to the second-order quantities with respect to $\boldsymbol{\xi}$. Now, we consider a system consisting of a central object and a disk surrounding the central object. Perturbations are only on the disk and the self-gravity of the disk gas is neglected. That is, the gravitational potential, $\psi(\boldsymbol{r})$, comes from the central object, and there is no Eulerian perturbation of $\psi(\boldsymbol{r})$.[1]

To represent the Lagrangian variation of density, $\delta\rho$, by quantities up to the second-order ones with respect to $\boldsymbol{\xi}$, we need the equation of continuity. We assume here that the perturbations are adiabatic. Then, the Lagrangian variation of pressure, δp, can be expressed by quantities up to the second-order ones with respect to $\boldsymbol{\xi}$. Then, the nonlinear hydrodynamic equation describing adiabatic, Nonself-gravitating perturbations is written as, after lengthy manipulation,

$$\rho_0 \frac{\partial^2 \boldsymbol{\xi}}{\partial t^2} + 2\rho_0(\boldsymbol{u}_0 \cdot \nabla)\frac{\partial \boldsymbol{\xi}}{\partial t} + \boldsymbol{L}(\boldsymbol{\xi}) = \rho_0 \boldsymbol{C}(\boldsymbol{\xi}, \boldsymbol{\xi}), \tag{3}$$

---

[1] The Lagrangian formulation by Lynden-Bell and Ostriker (1967) is quite general, and the effects of self-gravity can be taken into account. In this paper, however, we neglect the effects of self-gravity, since we are interested in standard accretion disks.

where $\boldsymbol{L}(\boldsymbol{\xi})$ is a linear operator with respect to $\boldsymbol{\xi}$ and is (Lynden-Bell and Ostriker 1967)

$$\boldsymbol{L}(\boldsymbol{\xi}) = \rho_0(\boldsymbol{u}_0 \cdot \nabla)(\boldsymbol{u}_0 \cdot \nabla)\boldsymbol{\xi} + \rho_0(\boldsymbol{\xi} \cdot \nabla)(\nabla\psi_0) + \nabla\left[(1 - \Gamma_1)p_0\mathrm{div}\boldsymbol{\xi}\right]$$
$$-p_0\nabla(\mathrm{div}\boldsymbol{\xi}) - \nabla[(\boldsymbol{\xi} \cdot \nabla)p_0] + (\boldsymbol{\xi} \cdot \nabla)(\nabla p_0), \tag{4}$$

and $\rho_0(\boldsymbol{r})$ and $p_0(\boldsymbol{r})$ are the density and pressure in the unperturbed state, and Γ_1 is the barotropic index specifying the linear part of the relation between Lagrangian variations δp and $\delta\rho$, i.e., $(\delta p/p_0)_{\mathrm{linear}} = \Gamma_1(\delta\rho/\rho_0)_{\mathrm{linear}}$. The right-hand side of wave equation (3) represents the nonlinear terms, which consist of two parts, i.e., $\rho_0\boldsymbol{C} = \rho_0\boldsymbol{C}_\psi + \rho_0\boldsymbol{C}_{\mathrm{p}}$. The former comes from $-\rho_0\delta(\nabla\psi)$ in equation (1) and $\rho_0\boldsymbol{C}_p$ from $-\rho_0\delta(\nabla p/\rho)$. Here and hereafter, for simplicity, we consider the case of $\Gamma_1 = 1$. Then, we have (Kato 2004) (an expression for nonlinear terms in the general case of $\Gamma_1 \neq 1$ is given in appendix)

$$\rho_0\boldsymbol{C}_\psi = -\frac{1}{2}\rho_0\xi_i\xi_j\frac{\partial^2}{\partial r_i\partial r_j}(\nabla\psi_0) \tag{5}$$

and

$$\rho_0\boldsymbol{C}_{\mathrm{p}} = -\frac{\partial}{\partial r_i}\left(p_0\frac{\partial\xi_i}{\partial r_j}\nabla\xi_j\right). \tag{6}$$

3. Wave Energy and Work Done on Oscillations

We now assume that the disks are deformed from an axisymmetric steady state by some external or internal cause. The Lagrangian displacement associated with the deformation is denoted by $\boldsymbol{\xi}^{\mathrm{W}}(\boldsymbol{r}, t)$. The deformation may be time-periodic with frequency ω^{W} as $\boldsymbol{\xi}^{\mathrm{W}} = \exp(i\omega^{\mathrm{W}}t)\hat{\boldsymbol{\xi}}^{\mathrm{W}}(\boldsymbol{r})$. In order to avoid unnecessary complication, however, we take $\omega^{\mathrm{W}} = 0$, hereafter. The effects of non-zero ω^{W} can easily be taken into account in the final results. As the deformation, a warp will be most probable, but it is not only one candidate of possible deformation. A plane-symmetric one-armed spiral deformation is one of another possible candidates that excite disk oscillations, as discussed later.

Our purpose here is to examine how the behavior of disk oscillations are affected by the disk deformation. As shown below, some of oscillation modes are resonantly excited on deformed disks through nonlinear coupling with disk deformation. The nonlinear coupling processes are schematically shown in figure 1 of Kato (2004).

Here we consider a disk oscillation mode. The displacement vector associated with the oscillation is denoted by $\boldsymbol{\xi}$ with frequency ω, i.e., $\boldsymbol{\xi} = \exp(i\omega t)\hat{\boldsymbol{\xi}}(\boldsymbol{r})$, in the limit of no deformation of disks. The first step of the nonlinear interaction between the disk oscillation characterized by $(\omega, \hat{\boldsymbol{\xi}})$ and the deformation characterized by $(0, \hat{\boldsymbol{\xi}}^{\mathrm{W}})$ introduces two kinds of intermediate oscillations. Let us denote the displacement vector associated with these intermediate oscillations by $\boldsymbol{\xi}_\pm^{\mathrm{int}}[\equiv \exp(i\omega t)\hat{\boldsymbol{\xi}}_\pm^{\mathrm{int}}]$. In other words, we characterize the two intermediate oscillations by $(\omega, \hat{\boldsymbol{\xi}}_+^{\mathrm{int}})$ and $(\omega, \hat{\boldsymbol{\xi}}_-^{\mathrm{int}})$, where $\hat{\boldsymbol{\xi}}_+^{\mathrm{int}}$ represents the intermediate oscillations resulting from the coupling between $\hat{\boldsymbol{\xi}}$ and $\hat{\boldsymbol{\xi}}^{\mathrm{W}}$, while $\hat{\boldsymbol{\xi}}_-^{\mathrm{int}}$ does those resulting from the coupling between $\hat{\boldsymbol{\xi}}$ and

$\hat{\boldsymbol{\xi}}^{\mathrm{W}*}$, where the asterisk represents the complex conjugate. That is, $\hat{\boldsymbol{\xi}}_+^{\mathrm{int}}$ and $\hat{\boldsymbol{\xi}}_-^{\mathrm{int}}$ are described, respectively, by

$$-\omega^2 \rho_0 \hat{\boldsymbol{\xi}}_+^{\mathrm{int}} + 2i\omega\rho_0(\boldsymbol{u}_0 \cdot \nabla)\hat{\boldsymbol{\xi}}_+^{\mathrm{int}} + \boldsymbol{L}(\hat{\boldsymbol{\xi}}_+^{\mathrm{int}}) = \frac{1}{2}[\rho_0\boldsymbol{C}(\hat{\boldsymbol{\xi}},\hat{\boldsymbol{\xi}}^{\mathrm{W}}) + \rho_0\boldsymbol{C}(\hat{\boldsymbol{\xi}}^{\mathrm{W}},\hat{\boldsymbol{\xi}})]. \qquad (7)$$

$$-\omega^2 \rho_0 \hat{\boldsymbol{\xi}}_-^{\mathrm{int}} + 2i\omega\rho_0(\boldsymbol{u}_0 \cdot \nabla)\hat{\boldsymbol{\xi}}_-^{\mathrm{int}} + \boldsymbol{L}(\hat{\boldsymbol{\xi}}_-^{\mathrm{int}}) = \frac{1}{2}[\rho_0\boldsymbol{C}(\hat{\boldsymbol{\xi}},\hat{\boldsymbol{\xi}}^{\mathrm{W}*}) + \rho_0\boldsymbol{C}(\hat{\boldsymbol{\xi}}^{\mathrm{W}*},\hat{\boldsymbol{\xi}})]. \qquad (8)$$

Next, the second stage of the nonlinear coupling is considered, which is a feedback process returning to the original oscillation, $\boldsymbol{\xi}$, by $\boldsymbol{\xi}_+^{\mathrm{int}}$ (or $\boldsymbol{\xi}_-^{\mathrm{int}}$) interacting with $\boldsymbol{\xi}^{\mathrm{W}}$. The feedback is described by

$$-\omega^2 \rho_0 \hat{\boldsymbol{\xi}} + 2i\omega\rho_0(\boldsymbol{u}_0 \cdot \nabla)\hat{\boldsymbol{\xi}} + \boldsymbol{L}(\hat{\boldsymbol{\xi}}) = \frac{1}{2}[\rho_0\boldsymbol{C}(\hat{\boldsymbol{\xi}}_+^{\mathrm{int}},\hat{\boldsymbol{\xi}}^{\mathrm{W}*}) + \rho_0\boldsymbol{C}(\hat{\boldsymbol{\xi}}^{\mathrm{W}*},\hat{\boldsymbol{\xi}}_+^{\mathrm{int}})], \qquad (9)$$

in the case where the nonlinear coupling between $\hat{\boldsymbol{\xi}}_+^{\mathrm{int}}$ and $\hat{\boldsymbol{\xi}}^{\mathrm{W}}$ feedbacks to the original oscillation, $\boldsymbol{\xi}$. On the other hand, in the case where $\boldsymbol{\xi}_-^{\mathrm{int}}$ and $\boldsymbol{\xi}^{\mathrm{W}}$ couples to feedback to the original oscillation, the equation corresponding to equation (9) is

$$-\omega^2 \rho_0 \hat{\boldsymbol{\xi}} + 2i\omega\rho_0(\boldsymbol{u}_0 \cdot \nabla)\hat{\boldsymbol{\xi}} + \boldsymbol{L}(\hat{\boldsymbol{\xi}}) = \frac{1}{2}[\rho_0\boldsymbol{C}(\hat{\boldsymbol{\xi}}_-^{\mathrm{int}},\hat{\boldsymbol{\xi}}^{\mathrm{W}}) + \rho_0\boldsymbol{C}(\hat{\boldsymbol{\xi}}^{\mathrm{W}},\hat{\boldsymbol{\xi}}_-^{\mathrm{int}})]. \qquad (10)$$

An important point to be noted here is that as a result of this feedback process, the original disk oscillation is amplified or dampened, i.e., the frequency, ω, can be no longer real, since in the feedback a resonant process is involved as shown later. How much is the imaginary part of ω? This can be examined from equations (9) and (10) by using the fact that the operators $i\rho_0(\boldsymbol{u}_0 \cdot \nabla)$ and $\boldsymbol{L}$ are Hermitian (Lynden-Bell and Ostriker 1967).

Let us now multifly equation (9) by $\hat{\boldsymbol{\xi}}^{*}$ and integrate over the whole volume, and consider the imaginary part of the resulting equation. The volume integration of $\hat{\boldsymbol{\xi}}^{*} \cdot \boldsymbol{L}(\hat{\boldsymbol{\xi}})$ does not have any imaginary part, since the operator $\boldsymbol{L}$ is Hermitian. Now we write $\omega = \omega_0 + i\omega_i$, where ω_i is the imaginary part of ω. Then, from equation (9) we have

$$-2\omega_{\mathrm{i}} \int \rho_0\boldsymbol{\xi}^{*}[\omega_0 - i(\boldsymbol{u}_0 \cdot \nabla)]\boldsymbol{\xi} dV = \Im\frac{1}{2}\int \rho_0\hat{\boldsymbol{\xi}}^{*}[\boldsymbol{C}(\hat{\boldsymbol{\xi}}_+^{\mathrm{int}},\hat{\boldsymbol{\xi}}^{\mathrm{W}*}) + \boldsymbol{C}(\hat{\boldsymbol{\xi}}^{\mathrm{W}*},\hat{\boldsymbol{\xi}}_+^{\mathrm{int}})]dV. \qquad (11)$$

This equation has a clear physical meaning. The integral on the left-hand side is related to the wave energy. Really, the wave energy is expressed as (Kato 2001)

$$E = \frac{1}{2}\omega_0 \int \rho_0\hat{\boldsymbol{\xi}}^{*}[\omega_0 - i(\boldsymbol{u} \cdot \nabla)]\hat{\boldsymbol{\xi}} dV. \qquad (12)$$

The right-hand side of equation (11) is thus $-4(\omega_{\mathrm{i}}/\omega_0)E$. Hereafter, the subscript 0 to ω is neglected for simplicity. In the case of oscillations that have m-arms in the azimuthal direction in geometrically thin disks, the wave energy E can be expressed in terms of $\boldsymbol{\xi}$ as (Kato 2001)

$$E = \frac{1}{2}\int \omega(\omega - m\Omega)\rho_0(|\hat{\xi}_r|^2 + |\hat{\xi}_z|^2)dV, \qquad (13)$$

where the cylindrical coordinates (r, φ, z) whose origin is at the disk center and the z-axis is the axis of disk rotation have been introduced.

5

Next, the right-hand side of equation (11) is considered. This is related to the work done on oscillations. Let us assume that an external force $\boldsymbol{f}$ on the oscillations acts per unit volume. Then, the work done by the force on the oscillations per unit time, W, is

$$W = \langle \int \rho_0 \frac{\partial \boldsymbol{\xi}}{\partial t} \cdot \boldsymbol{f} dV \rangle, \tag{14}$$

where $\langle \ \rangle$ represents the time average. If we write $\boldsymbol{\xi} = \Re[\exp(i\omega t)\hat{\boldsymbol{\xi}}]$ and $\boldsymbol{f} = \Re[\exp(i\omega t)\hat{\boldsymbol{f}}]$, we find that W can be expressed as

$$W = \frac{\omega}{2} \Im \int \rho_0 \hat{\boldsymbol{\xi}}^* \cdot \hat{\boldsymbol{f}} dV. \tag{15}$$

This means that in the present case, i.e., equation (9), the work done on the original oscillations by the nonlinear coupling terms is

$$W_+ = \frac{\omega}{2} \Im \int \frac{1}{2} \rho_0 \hat{\boldsymbol{\xi}}^* [\boldsymbol{C}(\hat{\boldsymbol{\xi}}_+^{\mathrm{int}}, \hat{\boldsymbol{\xi}}^{\mathrm{W}*}) + \boldsymbol{C}(\hat{\boldsymbol{\xi}}^{\mathrm{W}*}, \hat{\boldsymbol{\xi}}_+^{\mathrm{int}})] dV, \tag{16}$$

where the subscript $+$ is attached to W in order to emphasize that the feedback occurs through $\hat{\boldsymbol{\xi}}_+^{\mathrm{int}}$. Hence, equation (11) can be expressed as

$$-\omega_{\mathrm{i},+} = \frac{W_+}{2E}, \tag{17}$$

which is an expected result.

In the case of the coupling through $\hat{\boldsymbol{\xi}}_-^{\mathrm{int}}$, the work done the original oscillations is written as

$$W_- = \frac{\omega}{2} \Im \int \frac{1}{2} \rho_0 \hat{\boldsymbol{\xi}}^* [\boldsymbol{C}(\hat{\boldsymbol{\xi}}_-^{\mathrm{int}}, \hat{\boldsymbol{\xi}}^{\mathrm{W}}) + \boldsymbol{C}(\hat{\boldsymbol{\xi}}^{\mathrm{W}}, \hat{\boldsymbol{\xi}}_-^{\mathrm{int}})] dV, \tag{18}$$

and

$$-\omega_{\mathrm{i},-} = \frac{W_-}{2E}. \tag{19}$$

The quantitities ω_{i}'s in equations (17) and (19) are different by difference of coupling path. In order to distinguish them, the subscript $+$ or $-$ is attached to ω_{i}.

The purpose in the following sections is thus to express $W_\pm$ more explicitly and to evaluate the sigh of $W_\pm$. It is noted that there are two cases where the wave energy is positive and negative. If the waves exist dominantly inside the corotation radius (i.e., the radius of $\omega = m\Omega$), the wave energy E is negative [see equation (13)] and a negative work ($W < 0$) leads to instability ($-\omega_{\mathrm{i}} > 0$), while the waves exist mainly outside the corotation radius, we have $E > 0$, and $W > 0$ leads to instability.

The coupling term $\boldsymbol{C}$ consists of two terms of $\boldsymbol{C}_\psi$ and $\boldsymbol{C}_{\mathrm{p}}$, given by equation (5) and (6), respectively. From equaion (5) we easily find that

$$\int \rho_0 \hat{\boldsymbol{\xi}}^* \boldsymbol{C}_\psi(\hat{\boldsymbol{\xi}}_+^{\mathrm{int}}, \hat{\boldsymbol{\xi}}^{\mathrm{W}*}) dV = \int \rho_0 \hat{\boldsymbol{\xi}}_+^{\mathrm{int}} \boldsymbol{C}_\psi(\hat{\boldsymbol{\xi}}^*, \hat{\boldsymbol{\xi}}^{\mathrm{W}*}) dV. \tag{20}$$

In the case of the integration of $\rho_0 \hat{\boldsymbol{\xi}}^* \boldsymbol{C}_{\mathrm{p}}$ over the volume, we perform two times the integration by part. Then, we have

6

$$\int \rho_0 \hat{\boldsymbol{\xi}}^* \boldsymbol{C}_{\mathrm{p}}(\hat{\boldsymbol{\xi}}_+^{\mathrm{int}}, \hat{\boldsymbol{\xi}}^{\mathrm{W}*}) dV = \int \rho_0 \hat{\boldsymbol{\xi}}_+^{\mathrm{int}} \boldsymbol{C}_{\mathrm{p}}(\hat{\boldsymbol{\xi}}^*, \hat{\boldsymbol{\xi}}^{\mathrm{W}*}) dV. \tag{21}$$

Hence, W_+ given by equation (16) is reduced to

$$W_+ = \frac{\omega}{2} \Im \int \frac{1}{2} \rho_0 \hat{\boldsymbol{\xi}}_+^{\mathrm{int}} [\boldsymbol{C}(\hat{\boldsymbol{\xi}}^*, \hat{\boldsymbol{\xi}}^{\mathrm{W}*}) + \boldsymbol{C}(\hat{\boldsymbol{\xi}}^{\mathrm{W}*}, \hat{\boldsymbol{\xi}}^*)] dV. \tag{22}$$

It is very important to note here that $\hat{\boldsymbol{\xi}}^*$, $\hat{\boldsymbol{\xi}}^{\mathrm{int}}$, and $\hat{\boldsymbol{\xi}}^{\mathrm{W}}$ in integrations (20) and (21) are commnesurable each other as one of their examples is shown above. This nature is not limited in the case of $\Gamma_1 = 1$. This holds generally even in the case of $\Gamma_1 \neq 1$, as shown in appendix. The terms in the brackets of equation (22) are just the complex conjugate of the right-hand side of equation (7), which makes the calculation of W_+ easy, as shown later.

In the case of the feedback through $\hat{\boldsymbol{\xi}}_-^{\mathrm{int}}$, we similarly have, from equation (18),

$$W_- = \frac{\omega}{2} \Im \int \frac{1}{2} \rho_0 \hat{\boldsymbol{\xi}}_-^{\mathrm{int}} [\boldsymbol{C}(\hat{\boldsymbol{\xi}}^*, \hat{\boldsymbol{\xi}}^{\mathrm{W}}) + \boldsymbol{C}(\hat{\boldsymbol{\xi}}^{\mathrm{W}}, \hat{\boldsymbol{\xi}}^*)] dV. \tag{23}$$

The terms in the brackets are just the complex conjugate of the right-hand side of equation (8), which makes the calculation of W_- easy, as in the case of W_+.

4. Dispersion Relation

Hereafter we restrict our attention to oscillations in geometrically thin disks. The steady unperturbed disks are assumed to be axially-symmetric and to have no motion except for rotation. Here, cylindrical coordinates (r, φ, z) are employed, in which the z-axis is perpendicular to the disk plane and the origin of the coordinates is at the disk center. The rotation is then described as $\boldsymbol{u}_0 = (0, r\Omega(r), 0)$. When we need numerical figures, we adopt the Keplerian form of Ω, i.e., $\Omega = \Omega_{\mathrm{K}}$, since geometrically thin disks are considered.

The oscillations that we consider here are assumed to have m arms in the azimuthal direction, i.e., $\hat{\boldsymbol{\xi}} \propto \exp(-im\varphi)$. We further assume that the radial wavelength of the oscillations is moderately short, and the local approximation in the radial direction can be adopted. That is, $\hat{\boldsymbol{\xi}} \propto \exp(ikr)$ and the radial variations of physical quantities in the unperturbed state are neglected compared with the radial variation of $\hat{\boldsymbol{\xi}}$. Concerning the vertical direction, however, we cannot adopt local approximations, since the disk is geometrically thin.

For mathematical simplicity, we assume that the disks are vertically isothermal. In the vertically isothermal disks the density $\rho_0(r, z)$ is stratified as (e.g., Kato et al. 1998)

$$\rho_0(r, z) = \rho_{00}(r) \exp\left[-\frac{z^2}{2H^2(r)}\right], \tag{24}$$

where ρ_{00} is the density on the equatorial plane, and H is the half-thickness of the disk and is related to the vertical epicyclic frequency, $\Omega_\perp$, by

$$\Omega_\perp^2 H^2 = \frac{p_0}{\rho_0} = c_{\mathrm{s}}^2(r). \tag{25}$$

The vertical epicyclic frequency, $\Omega_\perp$, is equal to the angular velocity of the Keplerian rotation, Ω_{K}, in the case of the central object being non-rotating, and practically equal to Ω, since the

disk is assumed to be geometrically thin. Hereafter, however, we use $\Omega_\perp$ without using Ω_K or Ω, so that we can trace back the effects of $\Omega_\perp$ on the final results. Furthermore, we assume that oscillations also occur isothermally. Then, we can neglect the term of $\nabla[(1-\Gamma_1)p_0\mathrm{div}\boldsymbol{\xi}]$ in the operator $\boldsymbol{L}$ in equation (4). Under these approximations, we express the r-, φ-, and z-components of the homogeneous parts of wave equation (3). Then, we have

$$[-(\omega-m\Omega)^2+\kappa^2-4\Omega^2+k^2c_s^2]\hat{\xi}_r - i2\Omega(\omega-m\Omega)\hat{\xi}_\varphi - ik\left(c_s^2\frac{\partial\hat{\xi}_z}{\partial z} - z\Omega_\perp^2\hat{\xi}_z\right) = 0, \quad (26)$$

$$-(\omega-m\Omega)^2\hat{\xi}_\varphi + i2\Omega(\omega-m\Omega)\hat{\xi}_r = 0, \quad (27)$$

$$-(\omega-m\Omega)^2\hat{\xi}_z - ikc_s^2\frac{\partial\hat{\xi}_r}{\partial z} - \left(c_s^2\frac{\partial^2\hat{\xi}_z}{\partial z^2} - \Omega_\perp^2 z\frac{\partial\hat{\xi}_z}{\partial z} - \Omega_\perp^2\hat{\xi}_z\right) = 0. \quad (28)$$

These wave equations are differential equations, and it is troublesome to rigorously solve these equations. In vertically isothermal disks, however, the wave equations can be approximately solved by separating r and z dependences of $\hat{\xi}$'s as, for example, $\hat{\xi}_r(r,z) = f(r)g(z/H)$, where f and g are some functions of r and z/H, respectively (Okazaki et al. 1987). Here, the functional form of $g(z/H)$ is determined by solving an eigenvalue problem describing the vertical behavior of the oscillations, and we have

$$g(z) \propto \mathcal{H}_n\left(\frac{z}{H}\right), \quad (29)$$

where $\mathcal{H}_n$ is the Hermite polynomial of argument z/H, and $n(=0,1,2,...)$ characterizes the number of node(s) of oscillations in the vertical direction. More explicitly, we have

$$\hat{\xi}_r(\boldsymbol{r}) = \breve{\xi}_{r,n}(r,\varphi)\mathcal{H}_n(z/H) \quad (30)$$

$$\hat{\xi}_\varphi(\boldsymbol{r}) = \breve{\xi}_{\varphi,n}(r,\varphi)\mathcal{H}_n(z/H), \quad (31)$$

$$\hat{\xi}_z(\boldsymbol{r}) = \breve{\xi}_{z,n}(r,\varphi)\mathcal{H}_{n-1}(z/H). \quad (32)$$

It is noted that the number of node(s) of $\hat{\xi}_z$ in the vertical direction is smaller than those of $\hat{\xi}_r$ and $\hat{\xi}_\varphi$ by one, as shown in equation (32). However, the subscript n (not $n-1$) is attached to $\breve{\xi}_z$ as $\breve{\xi}_{z,n}$ in order to emphasize that $\breve{\xi}_{r,n}$, $\breve{\xi}_{\varphi,n}$, and $\breve{\xi}_{z,n}$ are a set of solutions. The fact that the z-dependences of $\hat{\xi}_r$, $\hat{\xi}_\varphi$, and $\hat{\xi}_z$ given by equations (30) – (32) are really solutions of the set of equations (26) – (28) is found by substituting equations (30) – (32) into equations (26) – (28) and conforming that the right-hand side of equations (26) – (28) can be packed into terms proportional to $\mathcal{H}_n$, $\mathcal{H}_n$, and $\mathcal{H}_{n-1}$, respectively. The results are (Kato 2004)

$$[-(\omega-m\Omega)^2+\kappa^2-4\Omega^2+k^2c_s^2]\breve{\xi}_{r,n} - i2\Omega(\omega-m\Omega)\breve{\xi}_{\varphi,n} + i(kH)\Omega_\perp^2\breve{\xi}_{z,n} = 0, \quad (33)$$

$$-(\omega-m\Omega)^2\breve{\xi}_{\varphi,n} + i2\Omega(\omega-m\Omega)\breve{\xi}_{r,n} = 0, \quad (34)$$

$$[-(\omega-m\Omega)^2+n\Omega_\perp^2]\breve{\xi}_{z,n} - in(kH)\Omega_\perp^2\breve{\xi}_{r,n} = 0. \quad (35)$$

The solvability condition of these homogeneous equations is

$$D(\omega,m,n) \equiv [(\omega-m\Omega)^2-\kappa^2][(\omega-m\Omega)^2-n\Omega_\perp^2] - k^2c_s^2(\omega-m\Omega)^2 = 0. \quad (36)$$

This is the well-known local dispersion relation of oscillations characterized by ω, m, and n.

8

5. Expressions for Work Done on Oscillations and Stability Conditions

Our purpose here is to evaluate $W_\pm$ given by equations (22) and (23). As disk deformation, we consider two cases:

- case (i): $m^W = 1$ and $n^W = 1$.
- case (ii): $m^W = 1$ and $n^W = 0$.

The former is a warp and the latter is a one-armed pattern plane-symmetric with respect to the equatorial plane.

In both cases, for simplicity, the radial wavelength of the deformation is assumed to be rather long compared with the radial wavelength of the disk oscillations. That is, the radial variation of $\hat{\boldsymbol{\xi}}^W$ is neglected compared with that of $\hat{\boldsymbol{\xi}}$. For convenience, the part of the z-dependence of $\hat{\boldsymbol{\xi}}^W$ is separated from other parts as

$$\hat{\xi}_r^W(\boldsymbol{r}) = \breve{\xi}_r(r,\varphi)\mathcal{H}_{n^W}(z/H), \tag{37}$$

$$\hat{\xi}_\varphi^W(\boldsymbol{r}) = \breve{\xi}_\varphi(r,\varphi)\mathcal{H}_{n^W}(z/H), \tag{38}$$

$$\hat{\xi}_z^W(\boldsymbol{r}) = \breve{\xi}_z(r,\varphi)\mathcal{H}_{n^W-1}(z/H), \tag{39}$$

where $n^W = 1$ in case (i), and $n^W = 0$ and $\breve{\xi}_z$ is case (ii).

5.1. Inhomogeneous Wave Equation for Intermediate Oscillations

Nonlinear coupling between $\boldsymbol{\xi}$ and $\boldsymbol{\xi}^W$ introduces intermediate oscillations, represented by $\boldsymbol{\xi}^{int} = \exp(i\omega t)\hat{\boldsymbol{\xi}}^{int}$. Related to the fact that $\mathcal{H}_1\mathcal{H}_n = \mathcal{H}_{n+1} + n\mathcal{H}_{n-1}$, there are two major normal modes of intermediate oscillations induced by the coupling between oscillations and a warp. They are those characterized by $\mathcal{H}_{n+1}(z/H)$ and those characterized by $\mathcal{H}_{n-1}(z/H)$.[2] Concerning the φ-dependence of $\hat{\boldsymbol{\xi}}^{int}$, there are also two cases where $\hat{\boldsymbol{\xi}}^{int}$ is proportional to $\exp[-i(m+1)\varphi]$ and to $\exp[-(m-1)\varphi]$. That is, there are four modes of $\hat{\boldsymbol{\xi}}^{int}$ by differences of the φ- and z-dependences in the case of a warp. In order to treat these four modes separately, $\hat{\boldsymbol{\xi}}^{int}$ is written as

$$\hat{\xi}_r^{int}(\boldsymbol{r}) = \sum \breve{\xi}_{r,\pm,\tilde{n}}^{int}(r,\varphi)\mathcal{H}_{\tilde{n}}(z/H), \tag{40}$$

$$\hat{\xi}_\varphi^{int}(\boldsymbol{r}) = \sum \breve{\xi}_{\varphi,\pm,\tilde{n}}^{int}(r,\varphi)\mathcal{H}_{\tilde{n}}(z/H), \tag{41}$$

$$\hat{\xi}_z^{int}(\boldsymbol{r}) = \sum \breve{\xi}_{z,\pm,\tilde{n}}^{int}(r,\varphi)\mathcal{H}_{\tilde{n}-1}(z/H), \tag{42}$$

where the subscript $\pm$ is attached to $\breve{\xi}^{int}$ to represent the two cases where $\breve{\boldsymbol{\xi}}^{int}$ is proportional to $\exp[-i(m\pm1)\varphi]$ (see also section 3), and the subscript $\tilde{n}$ represents $n+1$ or $n-1$ in case (i) and $\tilde{n} = n$ in case (ii).

Now we solve inhomogeneous wave equation (7) of $\hat{\boldsymbol{\xi}}_+^{int}$. All the terms on the right-hand side of equation (7) have the φ-dependence of $\exp[-i(m+1)\varphi]$. Their z-dependences, however,

---

[2]   In case (ii), the z-dependence of the intermediate oscillations is $\mathcal{H}_n(z/H)$ alone.

are not always limited to $\mathcal{H}_{\tilde{n}}(z/H)$ nor $\mathcal{H}_{\tilde{n}-1}(z/H)$, although the major terms are those with such z-dependences. Here, we write the right-hand side of equation (7) as

$$\frac{1}{2}\rho_0[\boldsymbol{C}(\hat{\boldsymbol{\xi}},\hat{\boldsymbol{\xi}}^{\mathrm{W}}) + \boldsymbol{C}(\hat{\boldsymbol{\xi}}^{\mathrm{W}},\hat{\boldsymbol{\xi}})]_r = \rho_0 \sum_{\tilde{n}} \breve{A}_{r,+,\tilde{n}}(r,\varphi)\mathcal{H}_{\tilde{n}}(z/H) + \cdots \tag{43}$$

$$\frac{1}{2}\rho_0[\boldsymbol{C}(\hat{\boldsymbol{\xi}},\hat{\boldsymbol{\xi}}^{\mathrm{W}}) + \boldsymbol{C}(\hat{\boldsymbol{\xi}}^{\mathrm{W}},\hat{\boldsymbol{\xi}})]_\varphi = \rho_0 \sum_{\tilde{n}} \breve{A}_{\varphi,+,\tilde{n}}(r,\varphi)\mathcal{H}_{\tilde{n}}(z/H) + \cdots \tag{44}$$

$$\frac{1}{2}\rho_0[\boldsymbol{C}(\hat{\boldsymbol{\xi}},\hat{\boldsymbol{\xi}}^{\mathrm{W}}) + \boldsymbol{C}(\hat{\boldsymbol{\xi}}^{\mathrm{W}},\hat{\boldsymbol{\xi}})]_z = \rho_0 \sum_{\tilde{n}} \breve{A}_{z,+,\tilde{n}}(r,\varphi)\mathcal{H}_{\tilde{n}-1}(z/H) + \cdots, \tag{45}$$

and concentrate our attention on the terms shown by $\breve{A}$'s. Here, $+\cdots$ denotes other terms orthogonal both to $\mathcal{H}_{\tilde{n}}$ and $\mathcal{H}_{\tilde{n}-1}$, and the subscript $+$ is added to $\breve{A}$'s in order to emphasize that they have the φ-dependence of $\exp[-i(m+1)\varphi]$.

Under these preparations, we obtain from equation (7) equations describing $\breve{\xi}_{r,+,\tilde{n}}$, $\breve{\xi}_{\varphi,+,\tilde{n}}$, and $\breve{\xi}_{z,+,\tilde{n}}$ as [cf., equations (33) – (35)]

$$\left\{-[(\omega-(m+1)\Omega]^2 + \kappa^2 - 4\Omega^2 + k^2 c_{\mathrm{s}}^2\right\}\breve{\xi}_{r,+,\tilde{n}}^{\mathrm{int}} - i2\Omega[\omega-(m+1)\Omega]\breve{\xi}_{\varphi,+,\tilde{n}}^{\mathrm{int}}$$
$$+i(kH)\Omega_\perp^2\breve{\xi}_{z,+,\tilde{n}}^{\mathrm{int}} = \breve{A}_{r,+,\tilde{n}}, \tag{46}$$

$$-[\omega-(m+1)\Omega]^2\breve{\xi}_{\varphi,+,\tilde{n}}^{\mathrm{int}} + i2\Omega[\omega-(m+1)\Omega]\breve{\xi}_{r,+,\tilde{n}}^{\mathrm{int}} = \breve{A}_{\varphi,+,\tilde{n}}, \tag{47}$$

$$\left\{-[(\omega-(m+1)\Omega]^2 + \tilde{n}\Omega_\perp^2\right\}\breve{\xi}_{z,+,\tilde{n}}^{\mathrm{int}} - i\tilde{n}(kH)\Omega_\perp^2\breve{\xi}_{r,+,\tilde{n}}^{\mathrm{int}} = \breve{A}_{z,+,\tilde{n}}, \tag{48}$$

where $\tilde{n} = n+1$ or $n-1$ in case (i), and $\tilde{n} = n$ in case (ii).

In the case of intermediate oscillations characterized by $\hat{\boldsymbol{\xi}}_-^{\mathrm{int}}$, we can derive similar equations as the above. That is, we denote the right-hand side of equation (8) by $\breve{\boldsymbol{A}}_-$ with similar expressions as equations (43) – (45). Then, as equations describing $\breve{\xi}_{r,-,\tilde{n}}$, $\breve{\xi}_{\varphi,-,\tilde{n}}$, and $\breve{\xi}_{z,-,\tilde{n}}$, we obtain the same equations as (46) – (48), respectively, except that $m+1$ is changed to $m-1$ and the subscript $+$ in all variables are now changed to the subscript $-$.

The equations describing the intermediate oscillations, i.e., equations (46) – (48), and the corresponding equations for $\breve{\boldsymbol{\xi}}_{-,\tilde{n}}^{\mathrm{int}}$ can easily be solved with respect to $\breve{\xi}_{r,\pm,\tilde{n}}$, $\breve{\xi}_{\varphi,\pm,\tilde{n}}$, and $\breve{\xi}_{r,\pm,\tilde{n}}$. The results show that they are expressed in a form of $N_\pm/D_\pm$, where N_+, for example, is some combination of $\breve{\boldsymbol{A}}_{+,\tilde{n}}$'s on the right-hand side of equations (46) – (48) and $D_\pm$ is

$$D_\pm(\omega, m\pm1, \tilde{n}) \equiv \left\{-[\omega-(m\pm1)\Omega]^2 + \kappa^2\right\}\left\{-[\omega-(m\pm1)\Omega]^2 + \tilde{n}\Omega_\perp^2\right\}$$
$$-[\omega-(m\pm1)\Omega]^2 k^2 c_{\mathrm{s}}^2. \tag{49}$$

5.2. Resonance

The appearance of $D_\pm$ in the denominator comes from the fact that the homogeneous wave equation for the intermediate oscillations gives the dispersion relation as the solvability condition and this is $D_\pm(\omega, m\pm1, \tilde{n}) = 0$. In other word, at the radius where $D_\pm(\omega, m\pm1, \tilde{n}) = 0$ is satisfied, the intermediate oscillations resonantly response to the external forces given by the

10

right-hand side of the wave equations. In the case of intermediate oscillations of $\check{\boldsymbol{\xi}}^{\text{int}}_{+,\tilde{n}}$, the external forcing terms are the right-hand sides of equations (46) – (48).

Since we are considering the cases where $k^2 c_{\text{s}}^2$ is much smaller than Ω^2 (i.e., geometrically thin disks), the last term of the expression for $D_{\pm}$ can be approximately neglected (particle approximation). This means that the resonance occurs at two radii. One occurs at a radius close to the radius where

$$[\omega - (m \pm 1)\Omega]^2 - \kappa^2 = 0 \qquad (\text{horizontal resonance}) \tag{50}$$

holds, and the other does at a radius where

$$[\omega - (m \pm 1)\Omega]^2 = \tilde{n}\Omega_{\perp}^2. \qquad (\text{vertical resonance}) \tag{51}$$

The former is called hereafter the horizontal resonance since the resonance occurs by horizontal motions, and the latter the vertical resonance since it occurs by vertical motions. Our purpose here is to evaluate the right-hand side of equation (22) and (23) in these two cases. In order to explicitly see the effects of resonance, we introduce variables $\check{\zeta}_{r,\pm,\tilde{n}}$, $\check{\zeta}_{\varphi,\pm,\tilde{n}}$, and $\check{\zeta}_{z,\pm,\tilde{n}}$ defined by

$$\check{\xi}^{\text{int}}_{r,\pm,\tilde{n}} = \frac{\check{\zeta}_{r,\pm,\tilde{n}}}{D_{\pm}}, \quad \check{\xi}^{\text{int}}_{\varphi,\pm,\tilde{n}} = \frac{\check{\zeta}_{\varphi,\pm,\tilde{n}}}{D_{\pm}}, \quad \check{\xi}^{\text{int}}_{z,\pm,\tilde{n}} = \frac{\check{\zeta}_{z,\pm,\tilde{n}}}{D_{\pm}}. \tag{52}$$

Then, considering that $(1/2)\rho_0[\boldsymbol{C}(\hat{\boldsymbol{\xi}}^*, \hat{\boldsymbol{\xi}}^{\text{W}*}) + \boldsymbol{C}(\hat{\boldsymbol{\xi}}^{\text{W}*}, \hat{\boldsymbol{\xi}}^*)]$ is just the complex conjugate of the right-hand side of inhomogeneous wave equation with respect to $\hat{\boldsymbol{\xi}}^{\text{int}}_+$ [see equation (7)], and that the inhomogeneous wave equations are explicitly written by equations (46) – (48), we have

$$\frac{1}{2}\rho_0 \hat{\boldsymbol{\xi}}^{\text{int}}_+ \cdot [\boldsymbol{C}(\hat{\boldsymbol{\xi}}^*, \hat{\boldsymbol{\xi}}^{\text{W}*}) + \boldsymbol{C}(\hat{\boldsymbol{\xi}}^{\text{W}*}, \hat{\boldsymbol{\xi}}^*)]$$

$$= \rho_0 \frac{1}{D_+^2}\Bigg[\Big\{-[\omega - (m+1)\Omega]^2 + \kappa^2 - 4\Omega^2 + k^2 c_{\text{s}}^2\Big\}\check{\zeta}_{r,+,\tilde{n}}\check{\zeta}^*_{r,+,\tilde{n}}$$

$$+ i2\Omega[\omega - (m+1)\Omega](\check{\zeta}_{r,+,\tilde{n}}\check{\zeta}^*_{\varphi,+,\tilde{n}} - \check{\zeta}^*_{r,+,\tilde{n}}\check{\zeta}_{\varphi,+,\tilde{n}})$$

$$+ i\tilde{n}k^2 c_{\text{s}}^2(-\check{\zeta}_{r,+,\tilde{n}}\check{\zeta}^*_{z,+,\tilde{n}} + \check{\zeta}^*_{r,+,\tilde{n}}\check{\zeta}_{z,+,\tilde{n}})$$

$$- [\omega - (m+1)\Omega]^2 \check{\zeta}_{\varphi,+,\tilde{n}}\check{\zeta}^*_{\varphi,+,\tilde{n}} - \Big\{[\omega - (m+1)\Omega]^2 - \tilde{n}\Omega_{\perp}^2\Big\}\check{\zeta}_{z,+,\tilde{n}}\check{\zeta}^*_{z,+,\tilde{n}}\Bigg]. \tag{53}$$

Our purpose here is to evaluate the imaginary part of the volume integration of the right-hand side of equation (53) to have an expression for W_+. As we see later, $D_{\pm}$ is proportional to $r - r_{\text{c}}$ near the resonant radius r_{c} of $D_{\pm} = 0$. Here, r_{c} is a function of ω, m, $\tilde{n}$. The terms in the brackets of equation (53) are all real at a glance. Hence, the radial integration of the right-hand side of equation (53) has no imaginary part, unless the terms in the brackets have terms proportional to D_+. If they have terms proportional to D_+, however, the right-hand side of equation (53) has terms proportional to $1/D_+$ with real coefficients. Since, $1/D_+$ is a pole in the complex r-plane, the radial integration of $1/D_+$ brings about an imaginary part, as carefully discussed later.

In the case of the horizontal resonance, we have

$$-[\omega-(m+1)\Omega]^2+\kappa^2+k^2c_{\rm s}^2 \sim \frac{D_+}{-\kappa^2+\tilde{n}\Omega_\perp^2}, \tag{54}$$

while in the case of the vertical resonance, we obtain

$$-[\omega-(m+1)\Omega]^2+\tilde{n}\Omega_\perp^2 \sim \frac{D_+}{\kappa^2-\tilde{n}\Omega_\perp^2}. \tag{55}$$

Under these considerations, we pick up only, from the right-hand side of equation (53), the terms which contribute to the imaginary part when they are integrated in the radial direction. Then, we have

$$\begin{aligned}
W_{\rm H,+} &= \frac{\omega}{2}\Im\int\frac{1}{2}\rho_0\hat{\boldsymbol{\xi}}_+^{\rm int}[\boldsymbol{C}(\hat{\boldsymbol{\xi}}^*,\hat{\boldsymbol{\xi}}^{\rm W*})+\boldsymbol{C}(\hat{\boldsymbol{\xi}}^{\rm W*},\hat{\boldsymbol{\xi}}^*)]dV \\
&= \frac{\omega}{2}\Im\int\rho_0\mathcal{H}_{\tilde{n}}^2\left(\frac{z}{H}\right)\frac{1}{D_{\rm H,+}}|\check{\zeta}_{r,+,\tilde{n}}|^2\frac{1}{-\kappa^2+\tilde{n}\Omega_\perp^2}dV \\
&= \frac{\omega}{2}(2\pi)^{3/2}\tilde{n}!\,\Im\int\frac{1}{D_{\rm H,+}}|\check{\zeta}_{r,+,\tilde{n}}|^2\frac{r\rho_{00}(r)H}{-\kappa^2+\tilde{n}\Omega_\perp^2}dr
\end{aligned} \tag{56}$$

for the horizontal resonance. The final equality is obtained by performing the vertical integration by using the nature of the Hermite polynomials. Here, the subscript H has been attached to W_+ and D_+ in order to emphasize that the horizontal resonance is now considered. In the case of the vertical resonance, we have

$$\begin{aligned}
W_{\rm V,+} &= \frac{\omega}{2}\Im\int\rho_0\hat{\boldsymbol{\xi}}_+^{\rm int}[\boldsymbol{C}(\hat{\boldsymbol{\xi}}^*,\hat{\boldsymbol{\xi}}^{\rm W})+\boldsymbol{C}(\hat{\boldsymbol{\xi}}^{\rm W},\hat{\boldsymbol{\xi}}^*)]dV \\
&= \frac{\omega}{2}\Im\int\rho_0\mathcal{H}_{\tilde{n}-1}^2\left(\frac{z}{H}\right)\frac{1}{D_{\rm V,+}}|\check{\zeta}_{z,+,\tilde{n}}|^2\frac{r\rho_{00}(r)H}{\kappa^2-\tilde{n}\Omega_\perp^2}dr \\
&= \frac{\omega}{2}(2\pi)^{3/2}(\tilde{n}-1)!\,\Im\int\frac{1}{D_{\rm V,+}}|\check{\zeta}_{z,+,\tilde{n}}|^2\frac{r\rho_{00}(r)H}{\kappa^2-\tilde{n}\Omega_\perp^2}dr,
\end{aligned} \tag{57}$$

where the subscript V has been attached to W_+ and D_+ in order to clearly show that the vertical resonance is considered. It is noted that in the case of the vertical resonance, W, is proportional to $(\tilde{n}-1)!$, not $\tilde{n}!$.

In the case of coupling through $\hat{\boldsymbol{\xi}}_-^{\rm int}$, we have similar expressions as the above. They are

$$W_{\rm H,-} = \frac{\omega}{2}(2\pi)^{3/2}\tilde{n}!\,\Im\int\frac{1}{D_{\rm H,-}}|\check{\zeta}_{r,-,\tilde{n}}|^2\frac{r\rho_{00}H}{-\kappa^2+\tilde{n}\Omega^2}dr \tag{58}$$

$$W_{\rm V,-} = \frac{\omega}{2}(2\pi)^{3/2}(\tilde{n}-1)!\,\Im\int\frac{1}{D_{\rm V,-}}|\check{\zeta}_{z,-,\tilde{n}}|^2\frac{r\rho_{00}H}{\kappa^2-\tilde{n}\Omega^2}dr. \tag{59}$$

It is noted that $\tilde{n}=n+1$ or $n-1$ in the case where the disk deformation is a warp [case (i)], while $\tilde{n}=n$ in the spiral deformation of disks which are symmetric with respect to the equatorial plane [case (ii)].

5.3. Integrations of $1/D$ around the Resonant Radius

The imaginary part of equations (56) – (59) comes from the integration around the resonant radius, since the radius is a pole of the integrant in the complex r-plane. To perform the integration around a pole, we must be careful. If the frequency of oscillations, ω, is taken

12

to be real, the pole is just on the real axis of r, and it is a problem what path we should take around the pole, when we make integration along the real r-axis. It is known in plasma physics, however, that the following procedure can satisfy the requirement of causality. That is, we perform the integration along the real r-axis, tentatively assuming that the oscillations in consideration are growing (i.e., $\omega_i < 0$ in the present problem), and then the results obtained in this way are analytically extended to the case of $\omega_i > 0$. Hereafter, we examine the horizontal and vertical resonance separately with this standard procedure.

(a) *Horizontal resonance*

For the horizontal resonance, we have $[\omega - (m \pm 1)\Omega]^2 - \kappa^2 \sim 0$ and around the resonant radius, r_c, the first term of the Tayor expansion of $D_{H,\pm}$ gives

$$D_{H,\pm} = 2(\tilde{n}\Omega_\perp^2 - \kappa^2)G_{H,\pm}\left[\frac{r - r_c}{r_c} - i\frac{\omega - (m \pm 1)\Omega_c}{G_{H,\pm}}\omega_i\right], \tag{60}$$

where

$$G_{H,\pm} = \left\{(m \pm 1)\Omega[\omega - (m \pm 1)\Omega]\frac{d\ln\Omega}{d\ln r} + \kappa^2\frac{d\ln\kappa}{d\ln r}\right\}_c, \tag{61}$$

and the subscript c denotes the values at the resonant radius. Considering these expressions and assuming $\omega_i < 0$ (the requirement of causality), we have (Kato 2004)

$$\int \frac{dr}{D_{H,\pm}} = -i\frac{\pi r_c}{2(\tilde{n}\Omega_\perp^2 - \kappa^2)_c|G_{H,\pm}|}\text{sign}[\omega - (m \pm 1)\Omega]_c. \tag{62}$$

It is noted that this result is valid even when $\omega_i > 0$ as mentioned before, although it is obtained under the assumption of $\omega_i < 0$.

Combining equations (56) [or (58)] and (62), we have, for horizontal resonance,

$$W_{H,\pm} = -\frac{\omega}{4}(2\pi)^{3/2}\pi\tilde{n}!\left[\frac{r^2\rho_{00}H}{(\tilde{n}\Omega_\perp^2 - \kappa^2)^2}\right]_c\frac{|\check{\zeta}_{r,\pm,\tilde{n}}|_c^2}{|G_{H,\pm}|}\text{sign}[\omega - (m \pm 1)\Omega]_c. \tag{63}$$

This result shows that the sign of the work done on the oscillations by the horizontal resonance is determined by the sign of $\omega - (m \pm 1)\Omega$ at the resonant radius. The work is positive if $\omega - (m \pm 1)\Omega$ at the resonant radius is negative.

(b) *Vertical resonance*

The work done on the oscillations by the vertical resonance is obtained by a similar way discussed above. That is, in the case of vertical resonance, the resonance occurs at a radius close to $[\omega - (m \pm 1)\Omega]^2 - \tilde{n}\Omega_\perp^2 = 0$. Around this resonant radius, r_c, we have

$$D_{V,\pm} = -2(\tilde{n}\Omega_\perp^2 - \kappa^2)G_{V,\pm}\left[\frac{r - r_c}{r_c} - i\frac{\omega - (m \pm 1)\Omega_c}{G_{V,\pm}}\omega_i\right], \tag{64}$$

where

$$G_{V,\pm} = \left\{(m \pm 1)\Omega[\omega - (m \pm 1)\Omega]\frac{d\ln\Omega}{d\ln r} + 2\tilde{n}\left(\Omega_\perp\frac{d\Omega_\perp}{d\ln r}\right)\right\}_c. \tag{65}$$

The radial integration of $1/D_{V,\pm}$ along the real r-axis then gives (Kato 2004)

13

$$\int \frac{dr}{D_{V,\pm}} = i\frac{\pi r_c}{2(\tilde{n}\Omega_\perp^2 - \kappa^2)_c|G_{V,\pm}|}\text{sign}[\omega - (m\pm 1)\Omega]_c. \tag{66}$$

Then, from equations (57) [or (59)] and (66), we have, for the vertical resonance,

$$W_{V,\pm} = -\frac{\omega}{4}(2\pi)^{3/2}\pi(\tilde{n}-1)!\left[\frac{r^2\rho_{00}H}{(\tilde{n}\Omega_\perp^2 - \kappa^2)^2}\right]_c \frac{|\check{\zeta}_{z,\pm,\tilde{n}}|^2_c}{|G_{V,\pm}|}\text{sign}[\omega - (m\pm 1)\Omega]_c. \tag{67}$$

It is noted that in the vertical resonance the sign of work done on oscillations is also determined by the sigh of $\omega - (m\pm 1)\Omega$ at the resonant radius. The radius of resonance is, however, different from that in the case of the horizontal resonance, although both radii of the horizontal and vertical resonances are simply denoted by the same symbol r_c, without distinguishing them.

5.4. *Stability Condition*

The wave energy given by equation (13) can be expressed as

$$E = \frac{(2\pi)^{3/2}}{2}\omega(\omega - m\Omega)_c(r^4 H\rho_{00})_c E_n, \tag{68}$$

where E_n is a dimensionless quantity given by

$$E_n = \int \frac{rH\rho_{00}}{(rH\rho_{00})_c}\frac{\omega - m\Omega}{(\omega - m\Omega)_c}\left(n!\frac{|\check{\xi}_r|^2}{r_c^2} + (n-1)!\frac{|\check{\xi}_z|^2}{r_c^2}\right)\frac{dr}{r_c}. \tag{69}$$

Hence, the growth rate, $-\omega_i$ [see equation (17) or (19)], can be expressed in the case of the horizontal resonance as

$$-\omega_{i,H,\pm} = -\frac{\pi}{4}\tilde{n}!\left[\frac{(\check{\zeta}_{r,\pm,\tilde{n}}/r)^2}{(\omega - m\Omega)(\tilde{n}\Omega_\perp^2 - \kappa^2)^2|G_{H,\pm}|}\right]_c \frac{\text{sign}[\omega - (m\pm 1)\Omega]_c}{E_n}. \tag{70}$$

Similarly, in the case of vertical resonance, we have from equation (67)

$$-\omega_{i,V,\pm} = -\frac{\pi}{4}(\tilde{n}-1)!\left[\frac{(\check{\zeta}_{z,\pm,\tilde{n}}/r)^2}{(\omega - m\Omega)(\tilde{n}\Omega_\perp^2 - \kappa^2)^2|G_{H,\pm}|}\right]_c \frac{\text{sign}[\omega - (m\pm 1)\Omega]_c}{E_n}. \tag{71}$$

The growth rates given by equations (70) and (71) show that the resonance leads to growth of oscillations when the sign of $[\omega - (m\pm 1)\Omega]/(\omega - m\Omega)$ at the resonant radius is negative. In the followings, we examine in what types of resonance and in what wave modes the sign becomes negative.

6. Resonant Radii and Resonant Frequencies of Locally Unstable Oscillations

This examination is separately made below for various combinations of types of resonance and of wave mode.

6.1. *Horizontal Resonance of Inertial-Acoustic or G-Mode Oscillations*

In the horizontal resonance, the resonance is realized at the radius where $[\omega - (m\pm 1)\Omega]^2 - \kappa^2 \sim 0$ [see equation (50)]. The inertial-acoustic or g-mode oscillations will be predominantly exist at the radius where $(\omega - m\Omega)^2 - \kappa^2 \sim 0$ is satisfied (see e.g., Kato and Fukue 2006). For

resonance to occur efficiently, both radii of $[\omega - (m \pm 1)\Omega]^2 = \kappa^2$ and $(\omega - m\Omega)^2 = \kappa^2$ must be the same. This condition is satisfied at the radius of

$$\kappa = \frac{\Omega}{2} \tag{72}$$

in two cases where

$$
\begin{aligned}
&\text{case (a)}: \omega - (m+1)\Omega = -\kappa \quad \text{and} \quad \omega - m\Omega = \kappa \\
&\text{case (b)}: \omega - (m-1)\Omega = \kappa \quad \text{and} \quad \omega - m\Omega = -\kappa.
\end{aligned} \tag{73}
$$

We see that in both cases the sign of $[\omega - (m+1)\Omega]/(\omega - m\Omega)$ or $[\omega - (m-1)\Omega]/(\omega - m\Omega)$ is negative. This implies that $-\omega_i > 0$ and the resonance amplifies the oscillations.

Let us see more in detail. In the former case of (a), $[\omega - (m+1)\Omega]_c < 0$ and the work done on the oscillations is positive [see equation (63)], and the wave energy is positive [see equation (68)]. Hence, the oscillations grow. In the latter case of (b), $[\omega - (m-1)\Omega]_c > 0$ and a negative work is done on the oscillations. The oscillations, however, grow since the wave energy is negative. Various quantities related to resonance and amplification are summarized in tables 1 and 2.

The above argument can be applied not only to the case where the disk is warped (i.e., $m^W = 1$ and $n^W = 1$), but also to the case where the disk is deformed by a one-armed pattern which is symmetric with respect to the equatorial plane (i.e., $m^W = 1$ and $n^W = 0$).

6.2. Horizontal Resonance of C-Mode or Vertical P-Mode Oscillations

These oscillation modes exist predominantly at the radius where $(\omega - m\Omega)^2 - n\Omega_\perp^2 \sim 0$. Both conditions of $[\omega - (m \pm 1)\Omega]^2 = \kappa^2$ and $(\omega - m\Omega)^2 = n\Omega_\perp^2$ can be simultaneously satisfied at the radius of

$$\kappa = n^{1/2}\Omega_\perp - \Omega. \tag{74}$$

when

$$
\begin{aligned}
&\text{case (a)}: \omega - (m+1)\Omega = \kappa \quad \text{and} \quad \omega - m\Omega = n^{1/2}\Omega_\perp \\
&\text{case (b)}: \omega - (m-1)\Omega = -\kappa \quad \text{and} \quad \omega - m\Omega = -n^{1/2}\Omega_\perp.
\end{aligned} \tag{75}
$$

This consideration shows that at the resonant point the sign of $[\omega - (m \pm 1)\Omega]/(\omega - m\Omega)$ is positive, showing that $-\omega_{i,H,\pm}$ given by equation (70) is negative. That is, the resonance dampens the oscillations (see tables 1 and 2).

6.3. Vertical Resonance of Inertial-Acoustic or G-Mode Oscillations

The condition of the vertical resonance is $[\omega - (m \pm 1)\Omega]^2 \sim \tilde{n}\Omega_\perp^2$. The radius where the inertial-acoustic or g-mode oscillations predominantly exists is $(\omega - m\Omega)^2 = \kappa^2$. Combination of these two relations shows that the resonance occurs at

$$\kappa = \tilde{n}^{1/2}\Omega_\perp - \Omega, \tag{76}$$

when

$$\text{case (a)} : \omega - (m-1)\Omega = \tilde{n}^{1/2}\Omega_\perp \quad \text{and} \quad \omega - m\Omega = \kappa$$

$$\text{case (b)} : \omega - (m+1)\Omega = -\tilde{n}^{1/2}\Omega_\perp \quad \text{and} \quad \omega - m\Omega = -\kappa. \tag{77}$$

In these two cases the sigh of $[\omega - (m\pm1)\Omega]/(\omega - m\Omega)$ is positive. Hence, equations (71) shows that the resonance dampens the oscillations.

The vertical resonance of c- and vertical p-mode oscillations is absent, since the conditions of $(\omega - m\Omega)^2 - \tilde{n}^{1/2}\Omega_\perp = 0$ and $(\omega - m\Omega)^2 - n^{1/2}\Omega_\perp = 0$ can not be simultaneously satisfied at any radius.

6.4. Rough Estimate of Growth Rate

Finally, the order of growth rate is briefly estimated in the case of horizontal resonance of inertial-acoustic or g-mode oscillations in warped disks. To do so, we must evaluate the order of $\breve{\xi}_r^{\text{int}}$. The nonlinear coupling terms between $\boldsymbol{\xi}$ and $\boldsymbol{\xi}^{\text{W}}$ are given by equations (5) and (6). Some detailed calculations show that the radial component of $\rho_0 \boldsymbol{C}_{\text{p}}$, for example, is on the order of $\rho_0 \xi_r \eta \Omega^2 (kH)/\lambda^{\text{W}}$ (Kato 2004), where ξ_r and η are the orders of the radial displacement associated with the oscillations and of the vertical displacement associated with the warp, respectively, and $1/k$ and λ^{W} are the radial wavelengths of the disk oscillation and the warp, respectively. Then, the wave equations describing the intermediate oscillations give the order of $\breve{\xi}_r^{\text{int}}$ as

$$\mathcal{O}(\breve{\xi}_r^{\text{int}}) = \frac{\xi_r \eta (kH)}{\lambda^{\text{W}}}. \tag{78}$$

Then, we have

$$\mathcal{O}(\breve{\zeta}_r^{\text{int}}) = \xi_r \eta \Omega^4 \frac{kH}{\lambda^{\text{W}}}. \tag{79}$$

The dimensionless wave energy contained in the disk, E_n, is found to be [see equation (69)]

$$\mathcal{O}(E_n) = \left(\frac{\xi_r}{r_{\text{c}}}\right)^2 \frac{L}{r_{\text{c}}}, \tag{80}$$

where L is the radial extend where the oscillations exist. Using these relations, we obtain from equation (70) that the growth rate is on the order of

$$\mathcal{O}(-\omega_{\text{i}}) = \alpha (kH)^2 \Omega, \tag{81}$$

where $\alpha = (\eta/\lambda^{\text{W}})^2 (r_{\text{c}}/L)$, confirming the results obtained by Kato (2004).[3]

7. Resonant Excitation of Global Oscillations

So far, we have considered resonant excitation of local oscillations, assuming that the oscillations are local in the radial direction in the sense that their radial wavelength is shorter

---

[3]   In Kato (2004), λ^{W} is taken to be r_{c}.

Table 1. Resonant oscillations in warped disks ($m^{\mathrm{W}} = 1$, $n^{\mathrm{W}} = 1$).

type of resonance	type of coupling	resonant radius	work	wave energy	stability
Inertial-acoustic mode and g-mode oscillations					
horizontal	$m \to m+1 \to m$	$r/r_{\mathrm{g}} = 4.0$	positive	positive	**growth**
	$m \to m-1 \to m$	$r/r_{\mathrm{g}} = 4.0$	negative	negative	**growth**
vertical	$m \to m+1 \to m$	$r/r_{\mathrm{g}} = 3.62,\ 6.46$	negative	positive	damping
	$m \to m-1 \to m$	$r/r_{\mathrm{g}} = 3.62,\ 6.46$	positive	negative	damping
c-mode and vertical p-mode oscillations					
horizontal	$m \to m+1 \to m$	$r/r_{\mathrm{g}} = 3.62,\ 6.46$	negative	positive	damping
	$m \to m-1 \to m$	$r/r_{\mathrm{g}} = 3.62,\ 6.46$	positive	negative	damping
vertical	absence				

Table 2. Resonant oscillations deformed by one-armed perturbations ($m^{\mathrm{W}} = 1$, $n^{\mathrm{W}} = 0$).

type of resonance	type of coupling	resonant radius	work	wave energy	stability
Inertial-acoustic mode and g-mode oscillations					
horizontal	$m \to m+1 \to m$	$r/r_{\mathrm{g}} = 4.0$	positive	positive	**growth**
	$m \to m-1 \to m$	$r/r_{\mathrm{g}} = 4.0$	negative	negative	**growth**
vertical	absence				
c-mode and vertical p-mode oscillations					
horizontal	absence				
vertical	absence				

than the characteristic radial scale-length of the disk (i.e., $kr > 1$). Certainly, we have extensively used the approximation in section 5 when the work done on oscillations is calculated. The processes of the analyses, however, suggest that the final result (i.e., the sign of the work done on oscillations by resonance is governed by the sign of $\omega - (m \pm 1)\Omega$ at the resonant radius [see equations (63) and (67)]) is free from the approximation, although the magnitude of the work depend on the radial form of oscillations. This anticipation seems to be supported by considering the other limit of the particle approximation ($kr > 1$), although it is not proved.

Different from the above, the resonant radii and resonant frequencies estimated in section 6 come from the approximation that the oscillations are local.[4] Thus, in this section we relax the approximation and examine how the results in section 6 are modified in cases of global oscillations.

---

[4] In section 6 we have assumed that the oscillations exist predominantly around the boundary of the propagation region, since the group velocity of the local oscillations vanishes there.

We restrict, however, our attention only to the case where oscillations are inertial-acoustic or g-mode oscillations and resonance is horizontal, since we can show that in other cases oscillations are damped or the resonance appears only in the evanescent region of the oscillations.

7.1. *Horizontal Resonance of Inertial-Acoustic Oscillations*

Let us consider inertial-acoustic oscillations of frequency ω with azimuthal wavenumber m. The propagation region of such inertial-acoustic oscillations is specified by $(\omega - m\Omega)^2 > \kappa^2$. In other words, the evanescent region of the oscillations is $(\omega - m\Omega)^2 < \kappa^2$, i.e., $m\Omega - \kappa < \omega < m\Omega + \kappa$. The evanescent regions in the ω–r plane (i.e., the so-called propagation diagram) are shown by dark area in figures 1 and 2 for $m = 1$ for $m = 2$, respectively. The region in the case of $m = 0$ is supplementarily shown in figure 3.

Next, we consider where the horizontal resonance occurs on the ω–r plane. In the coupling through $m \rightarrow m + 1 \rightarrow m$, the resonance occurs on the curve of $[\omega - (m+1)\Omega]^2 = \kappa^2$, while it occurs on the curve of $[\omega - (m-1)\Omega]^2 = \kappa^2$ in the coupling through $m \rightarrow m - 1 \rightarrow m$ [see subsection 5.2]. These curves are shown in figures 1 to 3 by thick (solid or dashed) or less thick dashed curves (see below for distinction of these curves).

The first problem to be examined is in which part of the curve of $[\omega - (m \pm 1)\Omega]^2 = \kappa^2$, resonance excites or dampens the oscillations. This can be examined by studying the sign of $[\omega - (m \pm 1)\Omega]/(\omega - m\Omega)$ on the curve [see that W's are given by equations (63) and (67) and the wave energy is given by equation (13)]. Above the curve of $\omega = m\Omega$ on the ω–r plane, the wave energy, E, is positive, while it is negative below the curve. Next, in the case of coupling through $m \rightarrow m + 1 \rightarrow m$, the sign of the work done on oscillations is governed by the sign of $\omega - (m+1)\Omega$. In the case of coupling through $m \rightarrow m - 1 \rightarrow m$, on the other hand, the sign of the work is governed by the sigh of $\omega - (m-1)\Omega$. Considering these situations, we find that resonance excites (amplifies) oscillations in the case where it occurs on the thick parts (including thick dashed parts) of the curves of $[\omega - (m \pm 1)\Omega]^2 = \kappa^2$. However, resonance leads to damping of oscillations in the case where the resonant point is on less thick dashed parts of the curves. These results are shown in figures 1 and 2 for $m = 1$ and $m = 2$, respectively, and supplementarily in figure 3 for $m = 0$.

Even when resonance excites oscillations, a strong excitation of the oscillations will not be expected in the case where the resonant point occurs in the evanescent region of the oscillations. This is because the coupling between the oscillations and the disk deformation is weak due to small amplitude of oscillations in the evanescent region. Hence, the parts of the curves of $[\omega - (m \pm 1)\Omega]^2 = \kappa^2$ where resonance excites oscillations but the resonance occurs in the evanescent region of oscillations are shown by thick and dashed curves.

As shown in figures 1 to 3, the thick solid parts of the resonant curves are only in a finite range of frequency. Propagations of some typical growing oscillations are shown in figures by

horizontal dashed lines. The resonant radius of these oscillations is shown by a large open circle on the lines. It is noted that the cases considered in section 6 under the local approximations are those where resonance is assumed to occur at the crossing point of the resonant curve and the boundary curve of the propagation region, i.e., at $4r_{\mathrm{g}}$.

The oscillations labeled by ω_{LL} in figure 1 and by ω_{L} in figure 2 are trapped in a finite range in radius, bounded between the inner edge of the disk ($\sim 3r_{\mathrm{g}}$) and the outer barrier of $\omega = \Omega - \kappa$ (for ω_{LL}) or of $\omega = 2\Omega - \kappa$ (for ω_{L}). Compared with these oscillations, the oscillations labeled by ω_{H} (figure 1) and ω_{HH} (figure 2) are not bounded in their outer boundary. In this sense, the latter two oscillations will be less observable with definite frequencies, compared with the former two ones. This consideration suggests that the pair QPOs observed in some X-ray binaries are the oscillations labeled by ω_{LL} and ω_{L} (see, e.g., Kato and Fukue 2006).

It is noted that in the limit of local perturbations, the oscillations labeled by ω_{LL} (figure 1) and ω_{L} (figure 2) tend to the oscillations of case (b) of equation (73). Similarly, the oscillations labeled by ω_{H} (figure 1) and ω_{HH} (figure 2) tend to the oscillations of case (a) of equation (73).

Finally, resonant excitation of axisymmmetric ($m = 0$) inertial-acoustic oscillations is briefly mentioned.[5] The results are shown in figure 3. In the case of $m = 0$, the resonance curve on the ω–r plane is $\omega = \Omega \pm \kappa$, and the evanescent region of the oscillations is the dark area below the curve of $\kappa(r)$. The same considerations as those in cases of $m = 1$ and $m = 2$ show that axisymmetric inertial-acoustic oscillations are excited in the case where resonance occurs on the curve of $\omega = \Omega - \kappa$. (On the thick dashed part of the curve, resonance occurs only in the evanescent region of the oscillations). The resonance on the curve of $\omega = \Omega + \kappa$ dampens oscillations (less thick dashed curve). The oscillations that can be excited by resonance are not trapped in a finite region. On the other hand, the oscillations whose frequencies are less than $\kappa_{\max}$ can be trapped, bounded inside by the inner edge of the disk and outside by the barrier of $\omega = \kappa$. Such oscillations, however, do not have resonance in their propagation region.
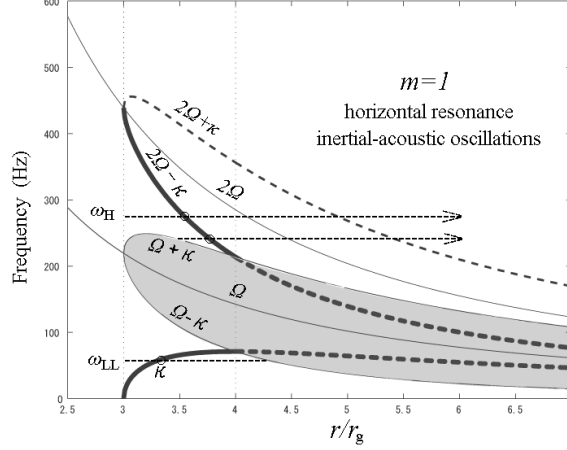
7.2. Horizontal Resonance of G-mode Oscillations

The frequency–radius relation where resonance occurs for g-mode oscillations with frequency ω and azimuthal wavenumber m is the same as that for inertial-acoustic oscillations with the same ω and m. On the curve of the frequency-radius relation, the part where resonance dampens g-mode oscillations is also the same as that in the case of inertial-acoustic oscillations.

A difference between inertial-acoustic oscillations and g-mode ones appears in their propagation regions. The propagation region of g-mode oscillations with frequency ω and azimuthal wavenumber m is $(\omega - m\Omega)^2 < \kappa^2$. That is, the evanescent regions of the inertial-acoustic oscillations (the shaded areas in figures 1, 2 and 3) are now the propagation regions of g-mode oscillations. That is, the shaded region in the figure is now the propagation region, and thus

---

[5]   So far, we less discussed the axisymmetric oscillations by assuming that they will not produce much light variation.

Fig. 1. Frequency–radius relation, $\omega = (m \pm 1)\Omega \pm \kappa$ (four combinations of $\pm$ being possible), showing resonant radii where inertial-acoustic oscillations with frequency ω and azimuthal wavenumber $m = 1$ have resonant interaction with disk deformation (thick solid, thick dashed, and less thick dashed curves). Horizontal resonance of inertial-acoustic oscillations is considered. In some part of the frequency-radius curve of $\omega = (m \pm 1) \pm \kappa$, the resonance excites inertial-acoustic oscillations, while in the other part the resonance dampens the oscillations. The part of excitation is shown by thick solid (or thick dashed) curves, while the part of damping is shown by a less thick dashed curve. Even in cases of excitation of oscillations, there are cases where the excitation occur in the evanescent region of the oscillations. Such cases are shown by thick but dashed curves, since the interaction between the oscillations and the deformation of disks is weak there. The evanescent region of $m = 1$ inertial-acoustic oscillations is shown as shaded area. For comparison, the curves of $\Omega(r)$ and $2\Omega(r)$ are also shown. The horizontal dashed curves demonstrate the propagation of typical oscillations that are excited. The open circles on the horizontal dashed curves show the radii where resonance occurs. The propagation of oscillations labeled by ω_{LL} is bounded in a finite range: The inner boundary is the inner edge of the disk and the outer boundary is the barrier of $\Omega - \kappa$. In the case of oscillations labeled by ω_{H}, the propagation region is bounded only in the inner boundary. In this sense, the latter oscillations labeled by ω_{H} will be less observable with a definite frequency, compared with the former oscillations of ω_{LL}.

the thick solid curve and the thick dashed one are interchanged.

This consideration shows that g-mode oscillations are trapped in a region with a finite radial extend, and in their propagation region, a resonance occurs so as to amplify the oscillations (see figures 1, 2 and 3). In the case of non-axisymmetric g-mode oscillations, however, we should remember the following situations. Except for the cases where the frequencies of g-mode oscillations are as high as the upper value limited by the propagation region of the oscillations, the corotation radius ($\omega = m\Omega$) appears in the propagation region of the oscillations (see figures 1 and 2). Different from the case of inertial-acoustic oscillations of $n = 0$, the presence of corotation resonance in the propagation region strongly dampens the g-mode oscillations (Kato 2003; Li et al. 2003). This strong damping suppresses the growth by the resonance by disk deformation considered here. In a narrow frequency range where the frequencies are as high

20
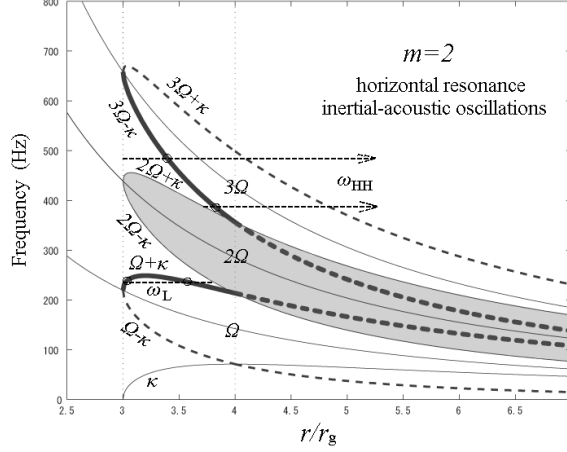
Fig. 2. The same as figure 1 except for $m = 2$. Because of the difference of m, the frequency–radius relation of resonance is now $\omega = \Omega \pm \kappa$ and $\omega = 3\Omega \pm \kappa$ (both signs of $\pm$ being possible). On the thick solid parts of the curves, resonance excites oscillations in their propagation region, but on the thick dashed part resonance occurs in the evanescent region of oscillations. The less thick dashed parts of the curves show the resonance that dampens inertial-acoustic oscillations. The evanescent region of the oscillations are now specified by $2\Omega - \kappa < \omega < 2\Omega + \kappa$ (dark area). For comparison, the curves of Ω, 2Ω, 3Ω are also shown. The propagation region of oscillations labeled by ω_{L} is bounded in a finite region. However, the region of oscillations labeled by ω_{HH} is not bounded in the outer region. In this sense, the latter oscillations will be less observable with a definite frequency, compared with the former oscillations with ω_{L}.

as the upper limit, the g-mode oscillations can be trapped in a radially narrow region without having corotation resonance in their propagation region (cf. figure 1). In this case, however, a resonance does not occur inside the propagation region (see figure 1).

To conclude, excitation (amplification) of global non-axisymmetric g-mode oscillations is less promising compared with that of global non-axisymmetric inertial-acoustic oscillations. Axisymmetric g-mode oscillations are, however, a good candidate of one of observed quasi-periodic oscillations. Axisymmetric g-mode oscillations are trapped around κ_{max} and excited, since a resonance that can excite the oscillations appears in the propagation region of the oscillations (see figure 3). This will be one of possible excitation mechanisms of the stable 67 Hz oscillation observed in GRS 1915+105.

8. Discussion

In this paper we have examined resonant excitation (amplification) of disk oscillations in deformed disks. Analyses are made in a general way as far as possible so that we can perspective see the essence of the resonant amplification processes.

In a previous paper (Kato 2004) we have considered a warp as a possible disk deformation to excite oscillations. In this paper, we show that, in addition to warps, a one-armed pattern symmetric with respect to the equatorial plane can also excite (amplify) disk oscillations.
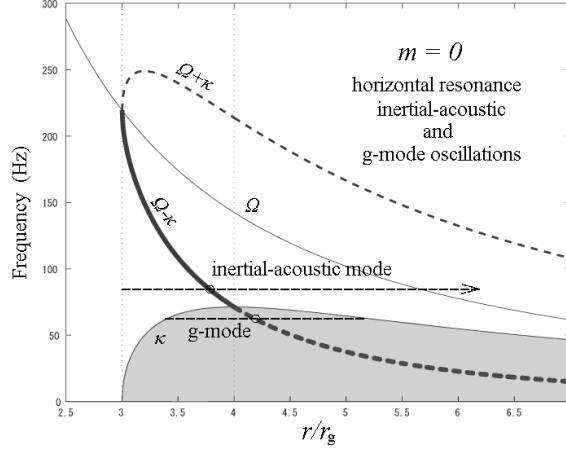
Fig. 3. The same as figure 1 except for $m = 0$. The dark area represents the evanescent region of inertial-acoustic oscillations (the propagation region of gravity oscillations). Oscillations with frequency of ω have resonance with disks at the radius where $\omega = \Omega \pm \kappa$ is satisfied. This frequency–radius relation is shown by separating into three parts; thick solid, thick dahsed, and less thick dashed parts. On the thick solid and thick dashed parts, resonance excites inertial-acoustic oscillations in their propagations region and in their evanescent region, respectively. (In the case of g-mode oscillations, the meaning of the thick solid part and the thick dashed one is exchanged.) On the less thick dashed part, resonance dampens inertial-acoustic oscillations. It is noted that trapped g-mode oscillations whose frequencies are around κ_{max} can be excited by our present resonant model.

As shown in the text, the horizontal resonance is of importance, since it can excite inertial-acoustic and g-mode oscillations. The resonance occurs at the radii of the resonant condition, $[\omega - (m \pm 1)\Omega]^2 = \kappa^2$, being satisfied, where ω and m are frequency and azimuthal wavenumber of inertial-acoustic (or g-mode) oscillations, respectively.

Important quantities determining the stability are, (i) the sign of work done by deformed disks to disk oscillations through resonance at resonant radius, and (ii) the sign of wave energy. As discussed in the text, the sign of the work done on the oscillations with ω and m is determined by the sign of $\omega - (m+1)\Omega$ [or $\omega - (m-1)\Omega$] at the resonant radius, depending that the path of coupling is $m \to m+1 \to m$ or $m \to m-1 \to m$. The sign of wave energy is determined where the corotation radius exists. If a wave is mainly inside the corotation radius of $\omega - m\Omega = 0$, the wave energy is negative, while it is positive when the main part of the wave is outside the corotation radius. By combination of the sign of the work done on waves and the sigh of the wave energy, excitation or damping of the waves is determined.

Whether resonance appears in the propagation region of oscillations or not is also important for observability of the oscillations. The propagation region of inertial-acoustic oscillations is specified by $(\omega - m\Omega)^2 > \kappa^2$, while that of the g-mode oscillations is $(\omega - m\Omega)^2 < \kappa^2$.

In this paper, some of the above results [i.e., the sign of work done on oscillations by resonance] are derived under the approximation that the oscillations are local in the sense that

22

their radial wavelength is shorter than the characteristic radial scale of disks (see section 5). The results, however, are free from the approximation, and valid even in the case of $kr < 1$.

The results mentioned so far restrict frequency ranges of resonantly excited oscillations, but their frequencies are not determined discretely or uniquely. Further restrictions concerning excited oscillations are made in section 6 by introducing assumptions that the oscillations are local and thus they are predominantly at the boundary of their propagation region, i.e., $(\omega - m\Omega)^2 \sim \kappa^2$. Results based on this assumption are summarized in tables 1 and 2 for two cases where the disk deformation is a warp (table 1) and it is a one-armed one plane-symmetric with respect to the disk plane (table 2). As shown in these tables, inertial-acoustic and g-mode oscillations are excited at the radius of $4r_{\rm g}$. Applications of these results to observed high-frequency QPOs are made, for example, by Kato and Fukue (2006), Kato (2007) and papers referred therein.

As mentioned before, unless the local approximation of oscillations is introduced, resonantly excited oscillations are not determined uniquely. What is determined is possible frequency range of excited oscillations. This issue is discussed in section 7 and the results are summarized in figures 1, 2 and 3. Eigenfunctions of global trapped oscillations will determine the most probable frequencies of resonantly excited oscillations. This problem, however, is outside the scope of this paper.

Finally, it is important to note that for the resonance considered in this paper to occur, the disk must be relativistic, i.e., otherwise, the resonant condition is not satisfied in the disk. In other words, for resonance to occur in relativistic disks, the disk deformation must be one-armed (i.e., a warp or one-armed pattern symmetric with respect to the equator).

Appendix A General Form of Nonlinear Coupling Terms

In general cases of $\Gamma_1 \neq 1$, the pressure coupling terms, $\boldsymbol{C}_{\rm p}$, given by equation (6) should be modified, although the term of $\boldsymbol{C}_\psi$ is unchanged. From equations (9)–(14) of Kato (2004), we have, after some manipulations,

$$\rho_0 C_{p,k}(\boldsymbol{\xi}, \boldsymbol{\xi}) = -\frac{\partial}{\partial r_i}\left(p_0 \frac{\partial \xi_i}{\partial r_j}\frac{\partial \xi_i}{\partial r_i}\right) + \frac{\partial}{\partial r_j}\left[(\Gamma_1 - 1)p_0 \frac{\partial \xi_j}{\partial r_k}\frac{\partial \xi_i}{\partial r_i}\right]$$
$$+\frac{1}{2}\frac{\partial}{\partial r_k}\left[(\Gamma_1 - 1)p_0 \frac{\partial \xi_i}{\partial r_j}\frac{\partial \xi_j}{\partial r_i}\right] + \frac{1}{2}\frac{\partial}{\partial r_k}\left[\Gamma_1(\Gamma_1 - 1)p_0 \frac{\partial \xi_i}{\partial r_i}\frac{\partial \xi_j}{\partial r_j}\right]. \tag{82}$$

Then, among $\boldsymbol{\xi}^{(1)}$, $\boldsymbol{\xi}^{(2)}$, and $\boldsymbol{\xi}^{(3)}$, such commnesurable relations as

$$\int \rho_0 \boldsymbol{\xi}^{(3)}\boldsymbol{C}_{\rm p}(\boldsymbol{\xi}^{(1)}, \boldsymbol{\xi}^{(2)})dV = \int \rho_0 \boldsymbol{\xi}^{(1)}\boldsymbol{C}_{\rm p}(\boldsymbol{\xi}^{(2)}, \boldsymbol{\xi}^{(3)})dV = \int \rho_0 \boldsymbol{\xi}^{(2)}\boldsymbol{C}_{\rm p}(\boldsymbol{\xi}^{(1)}, \boldsymbol{\xi}^{(3)})dV$$
$$= \cdots. \tag{83}$$

hold, where $\boldsymbol{\xi}^{(1)}$, $\boldsymbol{\xi}^{(2)}$, and $\boldsymbol{\xi}^{(3)}$ are arbitrary functions of $\boldsymbol{r}$. This can be shown by performing the integrations by parts, so that the integrands become symmetric with respect to $\boldsymbol{\xi}^{(1)}$, $\boldsymbol{\xi}^{(2)}$, and $\boldsymbol{\xi}^{(3)}$. This commensurable relation is a general nature of conservative systems. In the cases where varous perturbations are on a disk, energy exchange among these perturbations

23

may occur through resonant processes. The above commensurable relation, however, show that even in such cases, the total energy of perturbations is conserved in a conservative system. In other words, there is no spontaneous growth of perturbations in equilibrium disks. This is a reason why we consider deformed disks as the case of excitation of oscillations.

References

Abramowicz, M. A. & Kluźniak, W. 2001, A&A, 374, L19

Kato, S. 2001, PASJ, 53, 1

Kato, S. 2003, PASJ, 55, 257

Kato, S. 2003, PASJ, 55, 801

Kato, S. 2004, PASJ, 56, 905

Kato, S., & Fukue, J. 2006, PASJ 58, 909

Kato, S. 2007, PASJ 59, 451

Kato, S., Fukue, J., & Mineshige, S. 1998, Black-Hole Accretion Disks (Kyoto: Kyoto University Press), chap. 13

Kluźniak, W., & Abramowicz, M.A. 2001, Acta Phys. Pol. B32, 3605

Li, Li-Xin, Goodma, J., Narayan, R. 2003, ApJ, 593, 980

Lynden-Bell, D., & Ostriker, J. P. 1967, MNRAS, 136, 293

Okazaki, A. T., Kato, S., & Fukue, J. 1987, PASJ, 39, 457

Paczyński, B., & Wiita, P. J. 1980, A&A, 88, 23